Electronic Supplementary Material (ESI) for RSC Advances.

Supporting Information

Fourier-Transform Infrared and X-ray Diffraction Analyses of the Hydration Reaction of Pure Magnesium Oxide and Chemically Modified Magnesium Oxide

Ryo KUROSAWA [a], *Masato TAKEUCHI* [b] *and Junichi RYU* [a,*]

[a]Graduate School of Engineering, Chiba University, 1-33, Yayoi-cho, Inage-ku, Chiba, Japan

[b]Department of Applied Chemistry, Graduate school of Engineering, Osaka Prefecture University, 1-1, Gaku-en-cho, Naka-ku, Sakai, Osaka 599-8531, Japan

1. Experimental procedure

1.1. Reactivity evaluation for hydration reaction by using thermobalance

The reactivities of all the samples were determined using a thermobalance (TGD–9600 series, ADVANCE RIKO, Inc.). The samples (20 mg) were charged into a Pt cell. The mole fraction of $Mg(OH)_2$ was calculated based on the data obtained using the thermogravimetric (TG) analysis technique. A thermobalance was used during the process.[1–6]

The mole fraction was determined as follows:

$$x = \frac{(w_{ini} - w_{fin}) - (w_{ini} - w)}{(w_{ini} - w_{fin})}, \quad (1)$$

$$w_{fin} = w_{ini} \times \frac{M_{MgO}}{M_{Mg(OH)_2}}, \quad (2)$$

where w_{ini} represents the initial weight (the weight of $Mg(OH)_2$ at 200 ℃; [mg]), w_{fin} denotes the weight of $Mg(OH)_2$ that reacted (theoretical reaction; the weight of MgO; [mg]), w denotes the weight of $Mg(OH)_2$ in the sample during the reaction (mg), $M_{Mg(OH)2}$ is the molecular weight of $Mg(OH)_2$ [g mol^{-1}], M_{MgO} is the molecular weight of MgO [g mol^{-1}], and x denotes the mole fraction of $Mg(OH)_2$ [-]. We assumed that the added LiCl and LiOH were unreactive. The weights of LiCl and LiOH in the sample were subtracted from the total sample weight. [1–4,6]

Figure S1 shows the dehydration and hydration reaction profiles of $Mg(OH)_2$-W. x_0 [-] denotes the mole fraction of $Mg(OH)_2$ and was determined immediately before the sample was hydrated, x_h [-] denotes the mole fraction of the sample and the value was calculated immediately after hydration, and x_c [-] denotes the mole fraction of the sample determined 10 min after the completion of the hydration process. Δx_d, Δx_1, and Δx_2 [%] represent the extent of dehydration reaction conversion, hydration reaction conversion, and conversion change (physically adsorbed water), respectively (expressed as percentages) (**Figure S1**). These values are calculated as follows:

$$\Delta x_d = (1 - x_0) \times 100, \quad (3)$$

$$\Delta x_1 = (x_c - x_0) \times 100, \quad (4)$$

$$\Delta x_2 = (x_h - x_c) \times 100. \quad (5)$$

The temperature dependence of the hydration process (MgO hydration) was determined. T_h was varied (110, 170, and 200 ℃). Dehydration temperature (T_d) was set at 350 ℃ and the water vapor pressure was 57.8 or 31.2 kPa.

The non-zero mole fraction post dehydration can be potentially attributed to the presence of structural water. [7–9] The mole fraction (hydrated MgO) defined in this study denotes the net hydration conversion. The hydration behavior was studied (**Figure S2** and Eq. (6)). The mole fraction was determined as follows:

$$x_{hyd} = x - \Delta x_s, \quad (6)$$

where x_{hyd} [-] denotes the net change in the mole fraction due to hydration and Δx_s denotes the mole fraction of structural water.

2. Results

Figure S3 shows the Fourier transform-infrared (FT-IR) spectral profiles of L10. The spectrum of the as-prepared sample was recorded at room temperature (r. t.) in air. Following this, the sample was stored in the IR cell at r. t. in air. The storage time was varied as 10 min, 30 min, and 1 h,

following which the spectra were recorded. L10 was the sample of choice to study the effect of water as LiCl exhibited the property of deliquescence (in air). The intensities of the peaks at 3700, 3395, and 1634 cm^{-1}, which were assigned to the hydroxyl groups present on the surface of $Mg(OH)_2$, ν_{OH}, and δ modes of H_2O molecules adsorbed on the $Mg(OH)_2$ surface,[10] respectively, did not change significantly when they were exposed to air at r. t. for a period of 10–60 min (**Figure S3**). Thus, the water vapor present in the air barely influenced the FT-IR spectral profiles. The absorption band at 2359 cm^{-1} was assigned to CO_2 in the gas phase (**Figure S3**).[10] The absorption bands at 1523 and 1446 cm^{-1} could be ascribed to the CO_3^{2-} and/or HCO^{3-} species produced when CO_2 was adsorbed on the surface of MgO.[10,11] It was observed that the intensities of these bands did not change significantly. Diffraction patterns corresponding to carbonate species were not observed in the X-ray diffraction (XRD) patterns of the samples. It was observed that a small amount of carbonate was adsorbed on the sample surface. Fresh $Mg(OH)_2$ was exposed to a flow of CO_2 (flow rate: 100 $mL \cdot min^{-1}$; 24 h) at r. t. (referred to as CO_2-exposed $Mg(OH)_2$) to investigate the effect of CO_2 capture on the sample properties. A TAC1000SE thermobalance (Netzsch Japan, Inc., Japan) was used to conduct the experiments. **Figure S4** shows the hydration properties of fresh de-$Mg(OH)_2$-W and CO_2-exposed de-$Mg(OH)_2$. Both samples were dehydrated at 350 ℃ (time: 30 min) and then hydrated at 110 ℃ under an atmosphere of water vapor and Ar gas (mixture; 57.8 kPa; 80 min). The hydration properties of the samples were not significantly different from each other. These results revealed that the major constituent of the sample was MgO. It was also observed that surface carbonation did not influence the hydration behavior of MgO.

Figures S5–S7 show the hydration behaviors of de-$Mg(OH)_2$, de-L10, de-LO20, and de-L10/LO10 at 110, 170, and 200 ℃ under (P_{H2O}: 57.8 kPa). Analyses of the data presented in the figures reveal that the addition of Li compounds promotes the hydration of MgO. The co-addition of LiCl and LiOH enhanced the reactivity at 200 ℃. The data presented in **Figures S5–S7** were used to prepare **Figure S8**. The conversions of Δx_1 and Δx_2 were calculated using Eqs. (4) and (5), respectively.

Figure S9 shows the FT-IR spectral profile of de-MgO-W (before the hydration reaction at 110, 170, and 200 ℃). Two absorption bands at 3710 and 3691 cm^{-1} and a shoulder band at 3756 cm^{-1} were observed in this figure. These characteristic peaks were observed in the spectral profile of de-LO20 (before hydration; black lines in **Figures 7–9 (c)**). The results indicated that the surface state of de-LO20 was similar to that of MgO.

Figure S10 shows the FT-IR spectra recorded for $Mg(OH)_2$-W. [12–17] This peak assignment was the same as that in our previous study.[12] This figure was revised (**Figure 10**; main manuscript).

Figure S11 shows the hydration behavior of the de-$Mg(OH)_2$-W, de-L10, de-LO20, and de-L10/LO10 at 110 °C (P_{H2O}: 31.2 kPa). Initially, the mole fraction of $Mg(OH)_2$ (present in de-L10 and de-L10/LO10) increased rapidly. The increase could be attributed to the adsorption of water by LiCl. Under these conditions, the hydration of LiCl did not positively affect the hydration of MgO because the mole fraction of de-L10 (determined after an 80 min-long hydration process) was lower than the mole fraction of de-$Mg(OH)_2$-W.

Figure S12 shows the hydration behaviors of LiOH/MgO and de-$Mg(OH)_2$-W at 200 ℃. This figure shows that the hydration reactivity of LiOH/MgO increases with an increase in the amount

of LiOH. The data on hydration conversion (determined by analyzing the data presented here) has been presented in **Table S1**. A limited number of Mg^{2+} ion sites could be substituted by Li^{+} ions (**Figure S13**) because the peak at 3564 cm^{-1} (corresponding to $LiOH \cdot H_2O$) could not be detected in the spectra recorded with the impregnated LO20 sample. The results revealed that the hydration reactivity of MgO was influenced by the concentration of OH^{-} ions.

Figure S14 shows the FT-IR spectra recorded for hydrated de-MgO-W. The sample was hydrated at a temperature of 110 ℃ (P_{H2O}: 31.2 kPa).

References

(1) Ishitobi, H.; Uruma, K.; Takeuchi, M.; Ryu, J.; Kato, Y. Dehydration and hydration behavior of metal–salt–modified materials for chemical heat pumps. *Appl. Therm. Eng.* **2013**, *50*, 1639–1644.

(2) Ishitobi, H.; Hirao, N.; Ryu, J.; Kato, Y. Evaluation of heat output densities of lithium chloride–modified magnesium hydroxide for thermochemical energy storage. *Ind. Eng. Chem. Res.* **2013**, *52*, 5321–5325.

(3) Kurosawa, R.; Ryu, J. Effect of LiOH addition on dehydration reaction of $Mg(OH)_2$. *J. Chem. Eng. Jpn.* **2019**, *52*, 152–158.

(4) Kurosawa, R.; Takeuchi, M.; Ryu, J. Comparison of the effect of coaddition of Li compounds and addition of a single Li compound on reactivity and structure of magnesium hydroxide. *ACS Omega* **2019**, *4*, 17752–17761.

(5) Saitou, K.; Kurosawa, R.; Ryu, J. Dehydration and hydration reactivity of citrate-added $Mg(OH)_2$ for thermochemical energy storage. *Tetsu Hagané* **2020**, *106*, 546–555.

(6) Maruyama, A.; Kurosawa, R.; Ryu, J. Effect of lithium compound addition on the dehydration and hydration of calcium hydroxide as a chemical heat storage material. *ACS Omega* **2020**, *5*, 9820–9829.

(7) Kato, Y.; Yamashita, N.; Kobayashi, K.; Yoshizawa, Y. Kinetic study of the hydration of magnesium oxide for a chemical heat pump. *Appl. Therm. Eng.* **1996**, *16*, 853–862.

(8) Pimminger, H.; Habler, G.; Freiberger, N.; Abart, R. Evolution of nanostructure and specific surface area during thermally driven dehydration of $Mg(OH)_2$. *Phys. Chem. Minerals* **2016**, *43*, 59–68.

(9) Iwasaki, S.; Kodani, S.; Koga, N. Physico-geometrical kinetic modeling of the thermal decomposition of magnesium hydroxide. *J. Phys. Chem. C* **2020**, *124*, 2458–2471.

(10) Sivasankari, J.; Selvakumar, S.; Sivaji, K.; Sankar, S. Structural and optical characterization of MgO: X (X = Li, Na, and K) by solution combustion technique. *J. Alloys Compd.* **2014**, *616*, 51–57.

(11) Sutradhar, N.; Sinhamahapatra, A.; Roy, B.: Bajaj, H. C.; Mukhopadhyay, I.; Panda, A. B. Preparation of MgO nano-rods with strong catalytic activity via hydrated basic magnesium carbonates. *Mater. Res. Bull.* **2011**, *46*, 2163–2167.

(12) Kurosawa, R.; Takeuchi, M.; Ryu, J. Fourier-transform infrared analysis of the dehydration mechanism of $Mg(OH)_2$ and chemically modified $Mg(OH)_2$. *J. Phys. Chem. C* **2021**, *125*, 5559–5571.

(13) Anderson, P. J.; Horlock, R. F.; Oliver, J. F. Interaction of water with the magnesium oxide surface. *Trans. Faraday Soc.* **1965**, *61*, 2754–2762.

(14) Coluccia, S.; Marchese, L.; Lavagnino, S.; Anpo, M. Hydroxyls on the surface of MgO powders. *Spectrochim. Acta* **1987**, *43A*, 1573–1576.

(15) Knözinger, E.; Jacob, K. H.; Singh, S.; Hofmann, P. Hydroxyl groups as IR active surface probes on MgO crystallites. *Surf. Sci.* **1993**, *290*, 388–402.

(16) Chizallet, C.; Costentin, G.; Lauron-Pernot, H.; Krafft, J. M.; Bazin, P.; Saussey, J.; Delbecq, F.; Sautet, P.; Che, M. Role of hydroxyl groups in the basic reactivity of MgO: a theoretical and experimental study. *Oil Gas Sci. Technol.-Rev. IFP* **2006**, *61*, 479–488.

(17) Chizallet, C.; Costentin, G.; Che, M.; Delbecq, F.; Sautet, P. Infrared characterization of hydroxyl groups on MgO: A periodic and cluster density functional theory study. *J. Am. Chem. Soc.* **2007**, *129*, 6442–6452.

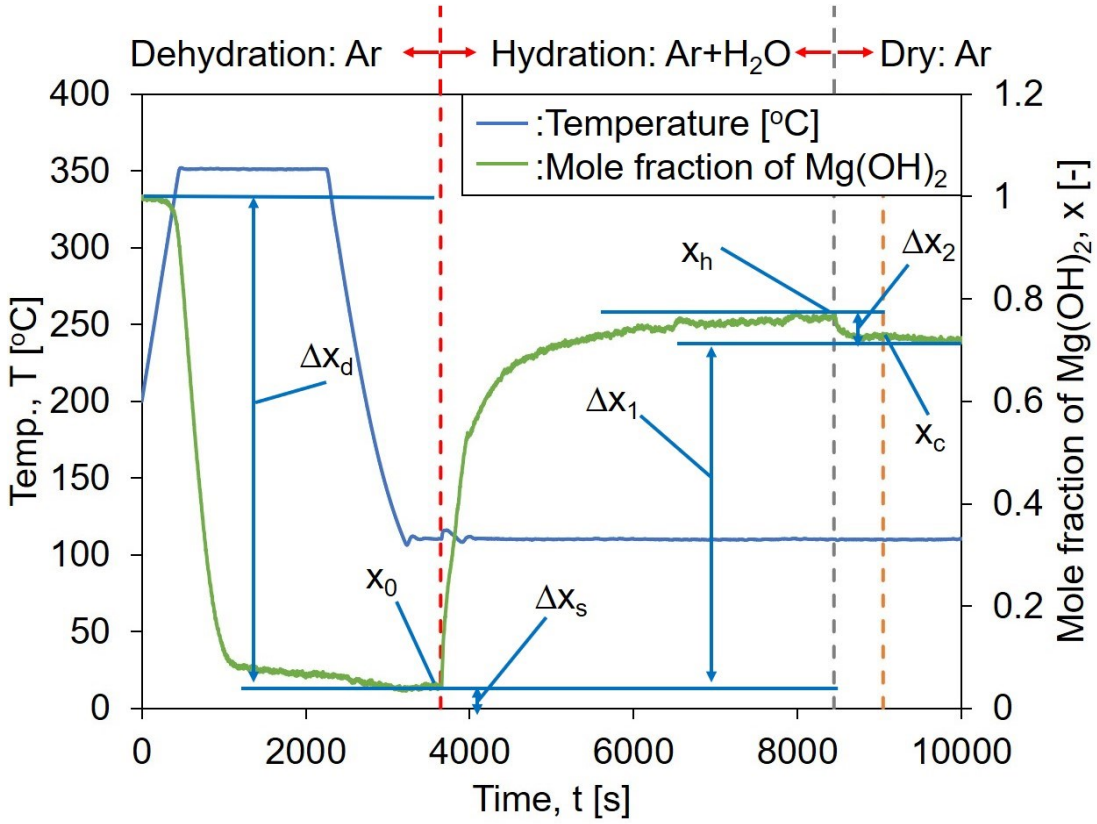

Figure S1. Dehydration and hydration reaction profiles of $Mg(OH)_2$-W (T_d = 350 ℃, T_h = 110 ℃, P_{H2O} = 57.8 kPa).

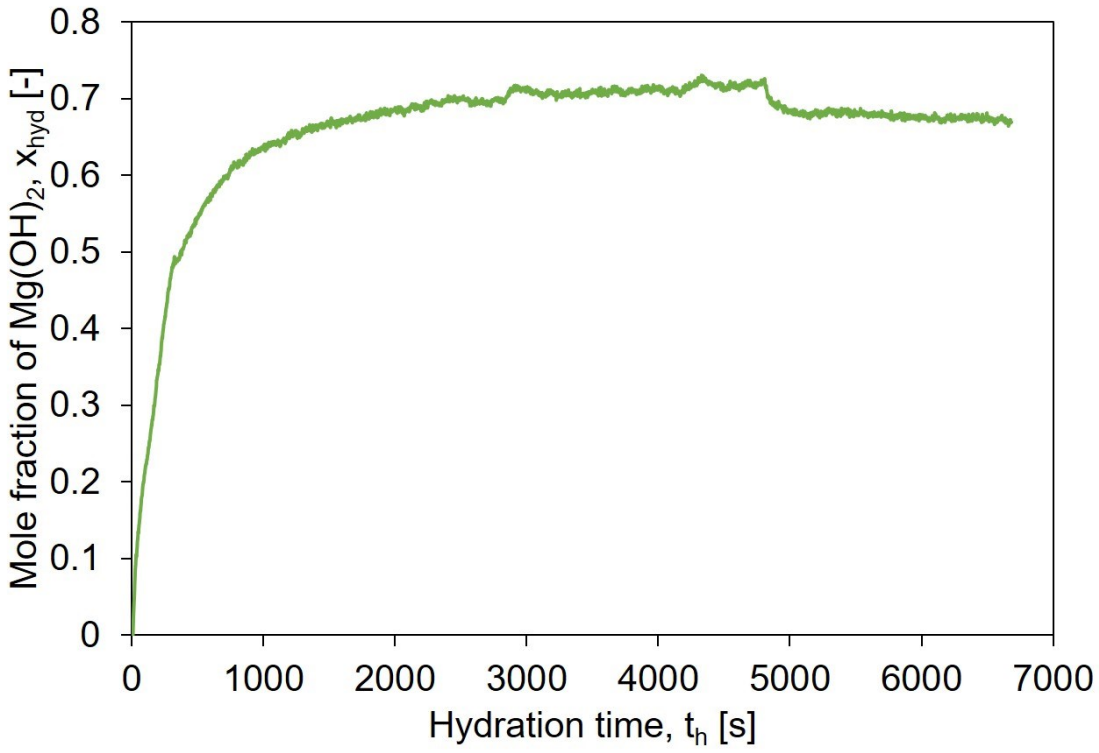

Figure S2. Hydration reaction profile of de-$Mg(OH)_2$-W studied at a temperature of 110 ℃ ($Mg(OH)_2$-W was dehydrated at 350 ℃, following which it was hydrated at 110 ℃ (P_{H2O}: 57.8 kPa)).

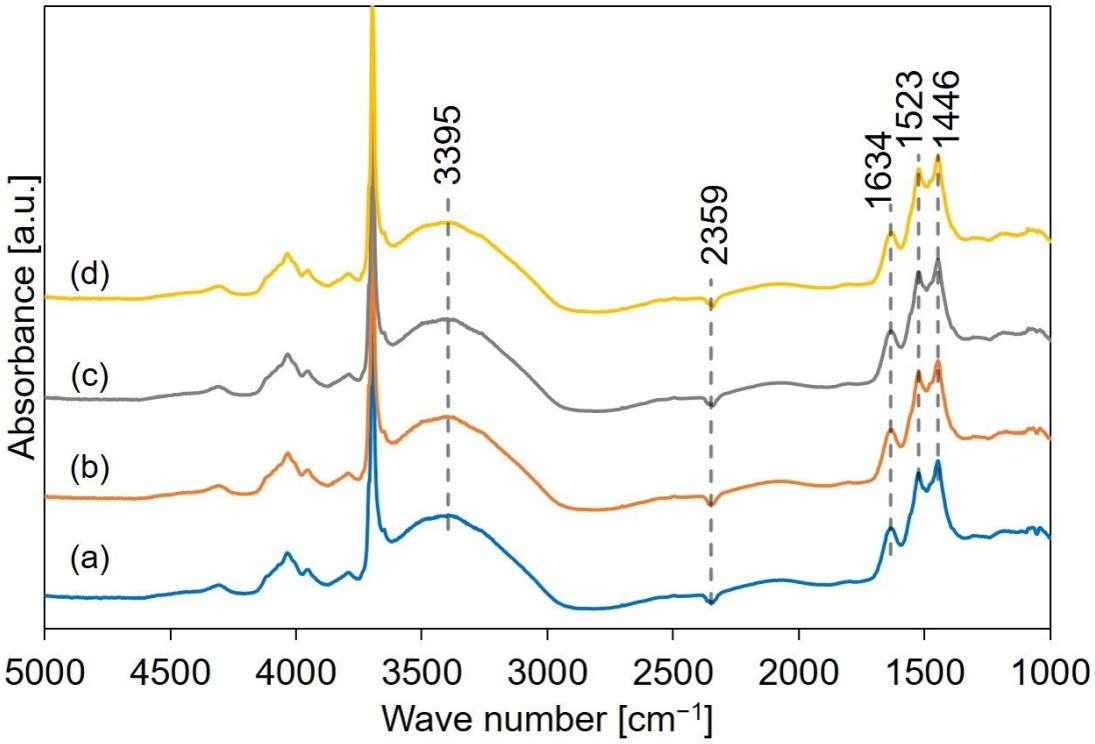

Figure S3. FT-IR spectral profile recorded for L10 (a) as-synthesized. The sample was stored in an IR cell at r. t. for (b) 10 min, (c) 30 min, and (d) 1 h. All the spectra were recorded under ambient conditions (in the air at r. t.), as described in the manuscript.

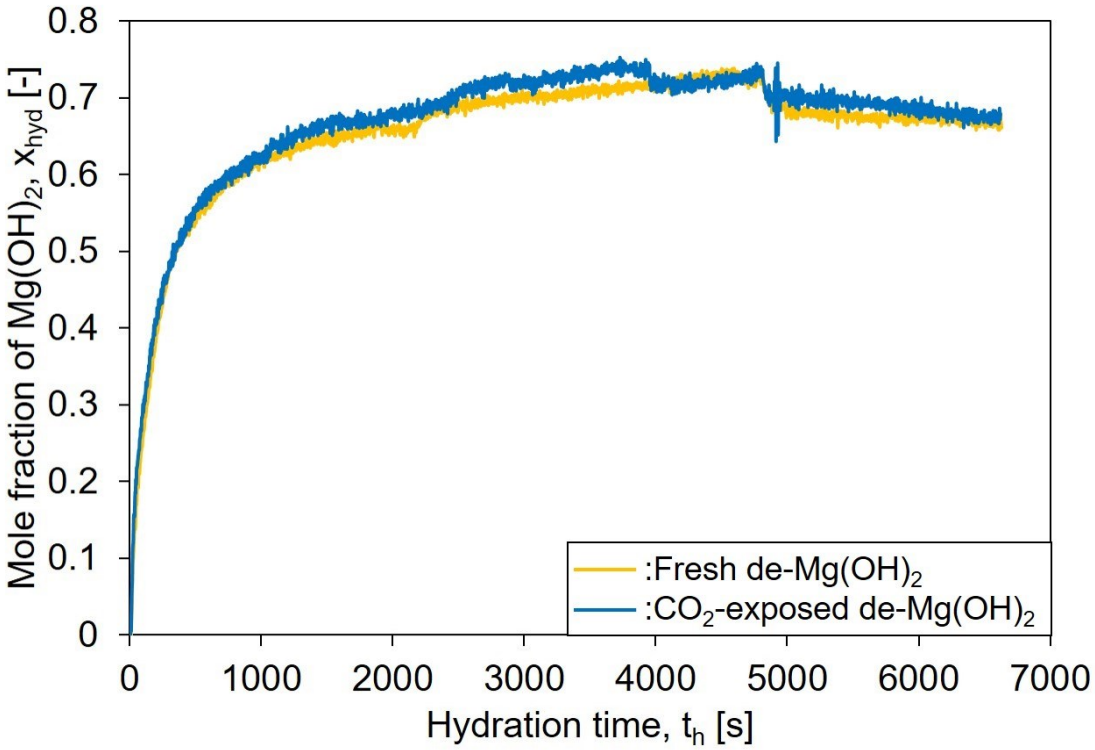

Figure S4. TG curves recorded for fresh de-$Mg(OH)_2$ and CO_2-exposed de-$Mg(OH)_2$. Fresh $Mg(OH)_2$ and CO_2-exposed $Mg(OH)_2$ samples were dehydrated at a temperature of 350 ℃, following which they were hydrated at 110 ℃ (P_{H2O}: 57.8 kPa).

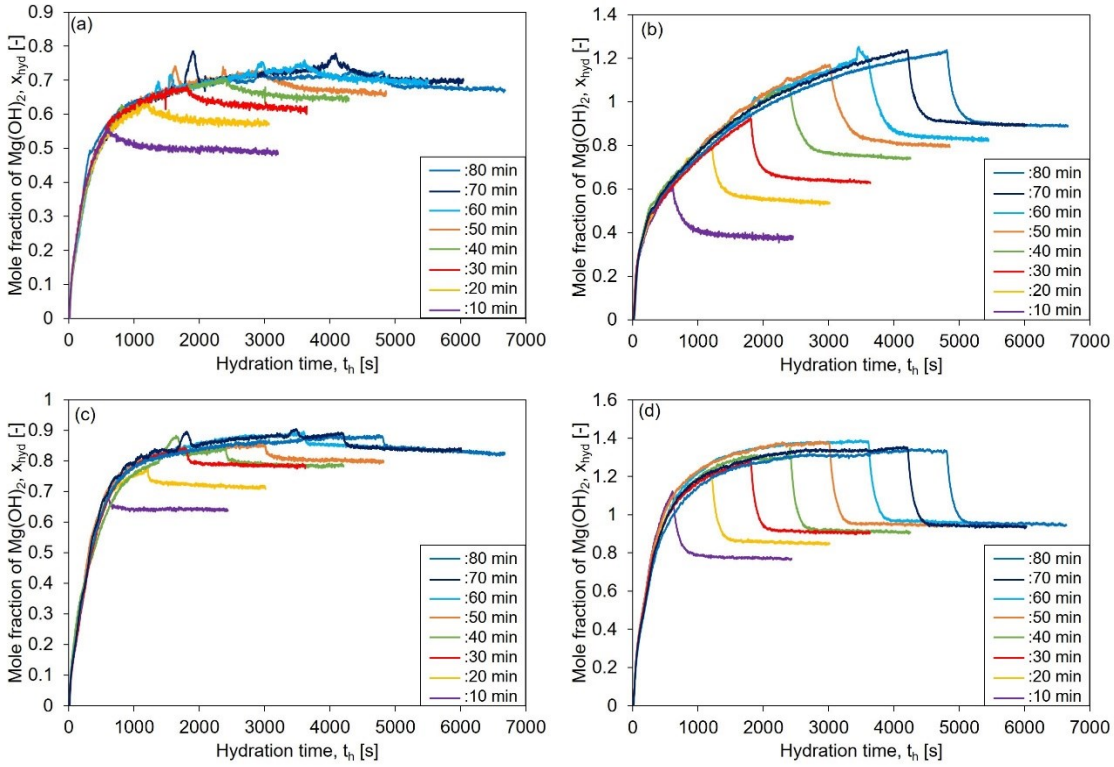

Figure S5. Hydration behavior of (a) de-$Mg(OH)_2$-W, (b) de-L10, (c) de-LO20, and (d) de-L10/LO10 studied at 110 ℃. $Mg(OH)_2$-W, L10, LO20, and L10/LO10 were dehydrated at 350 ℃, following which they were hydrated at 110 ℃ (P_{H2O}:57.8 kPa).

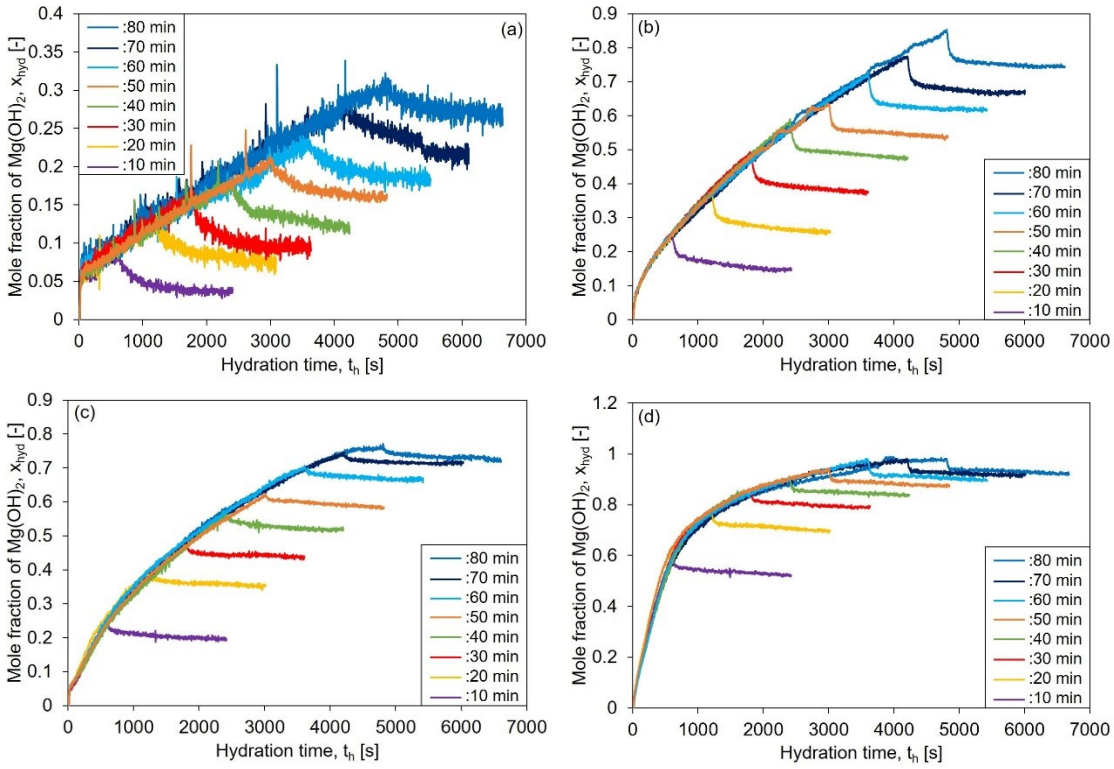

Figure S6. Hydration behavior of (a) de-$Mg(OH)_2$-W, (b) de-L10, (c) de-LO20, and (d) de-L10/LO10 studied at 170 ℃. $Mg(OH)_2$-W, L10, LO20, and L10/LO10 were dehydrated at 350 ℃, following which they were hydrated at 170 ℃ (P_{H2O}: 57.8 kPa).

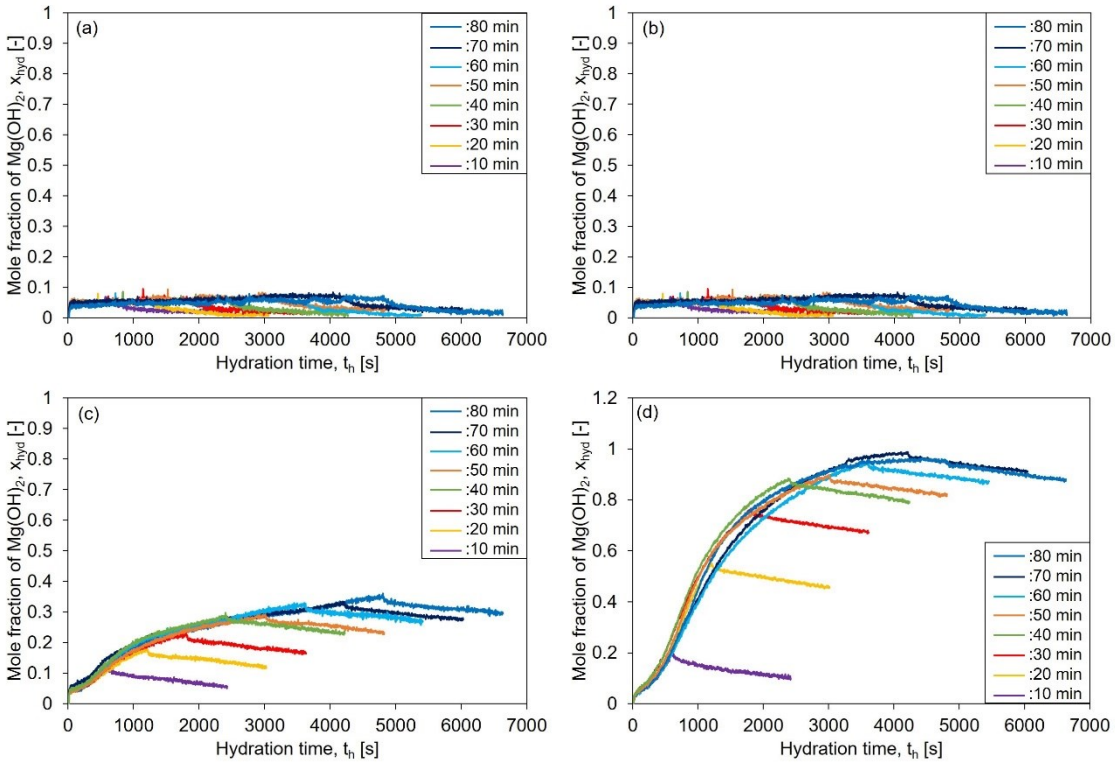

Figure S7. Hydration behavior of (a) de-$Mg(OH)_2$-W, (b) de-L10, (c) de-LO20, and (d) de-L10/LO10 studied at a temperature of 200 ℃. $Mg(OH)_2$-W, L10, LO20, and L10/LO10 were dehydrated at 350 ℃, following which they were hydrated at 200 ℃ (P_{H2O}: 57.8 kPa).

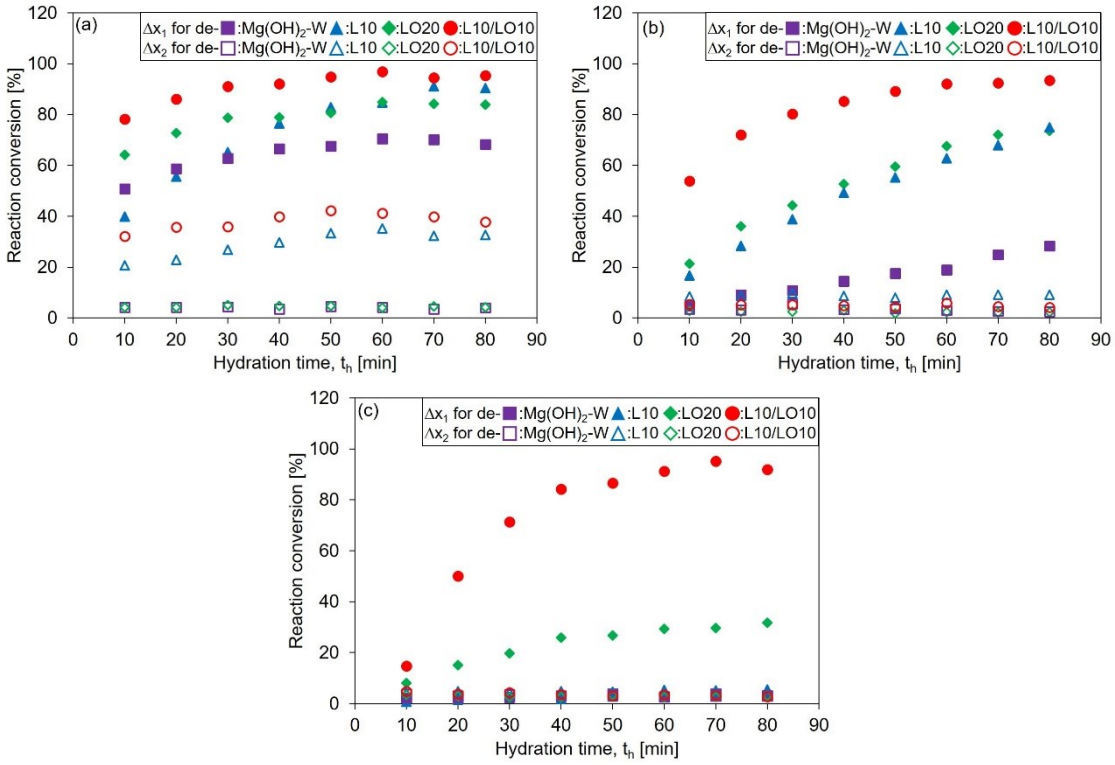

Figure S8. Reaction conversion *vs*. hydration time plots to determine the hydration reaction (Δx_1) and physical adsorption (Δx_2) values for dehydrated samples. Data were recorded at (a) 110 ℃, (b) 170 ℃, and (c) 200 ℃. Filled symbols and open symbols represent Δx_1 and Δx_2, respectively. $Mg(OH)_2$-W, L10, LO20, and L10/LO10 were dehydrated at a temperature of 350 ℃, following which they were hydrated at 110, 170, or 200 ℃ (P_{H2O}: 57.8 kPa).

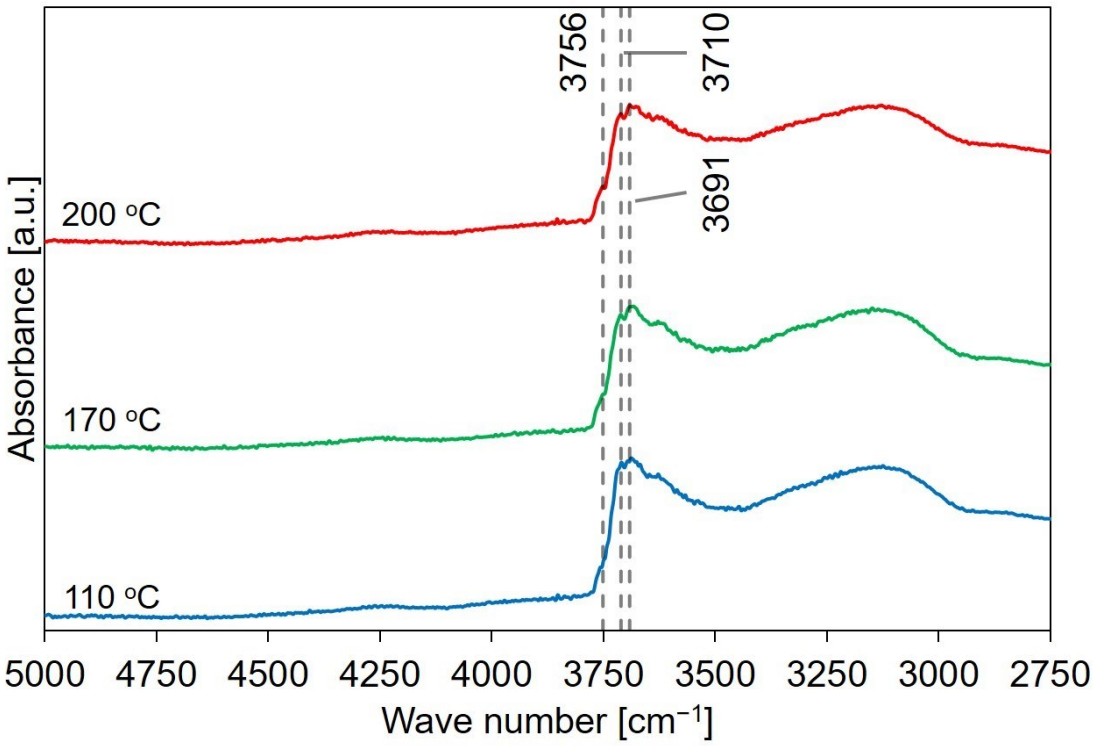

Figure S9. FT-IR spectral profiles of de-MgO-W. MgO-W was dehydrated at a temperature of 350 °C, following which it was dehydrated again at temperatures of 110, 170, and 200 ℃ for 10 min. (FT-IR spectral profiles were recorded at r. t. before the samples were hydrated).

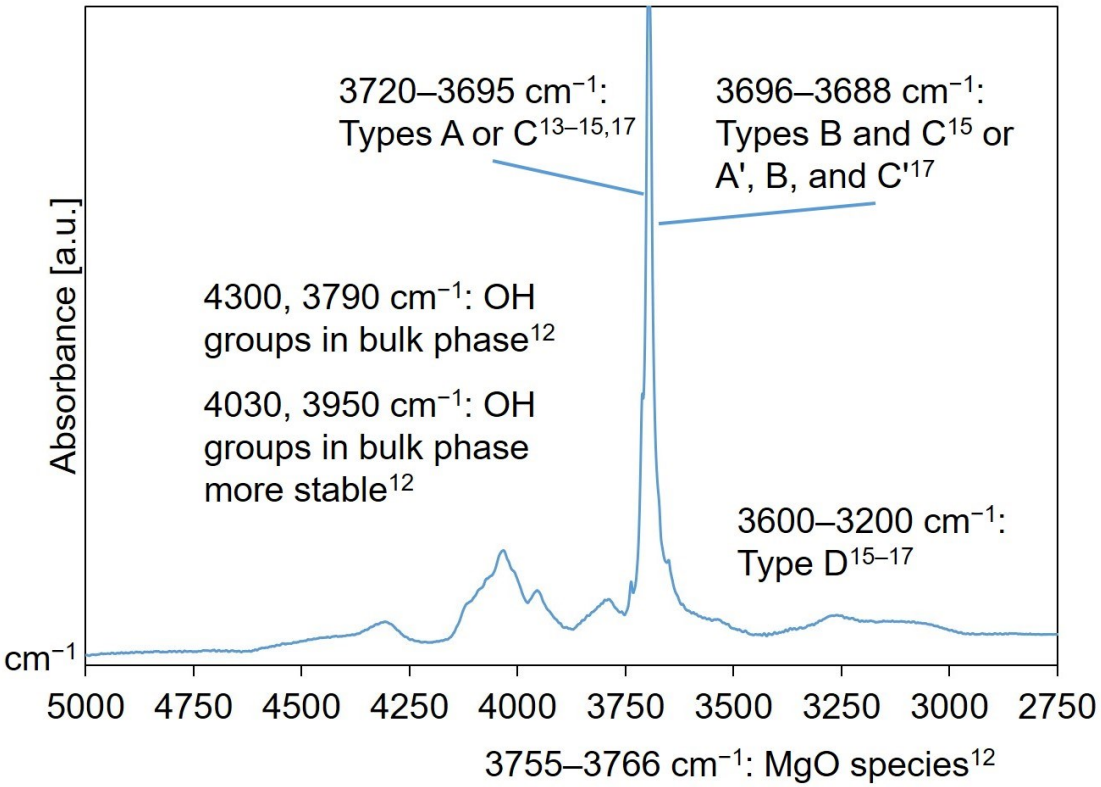

Figure S10. FT-IR spectral profiles of samples. Literature reports were referred to for peak assignment.[12–17] The peaks were reassigned, as shown in Figure 10. The data has been presented in the main manuscript.

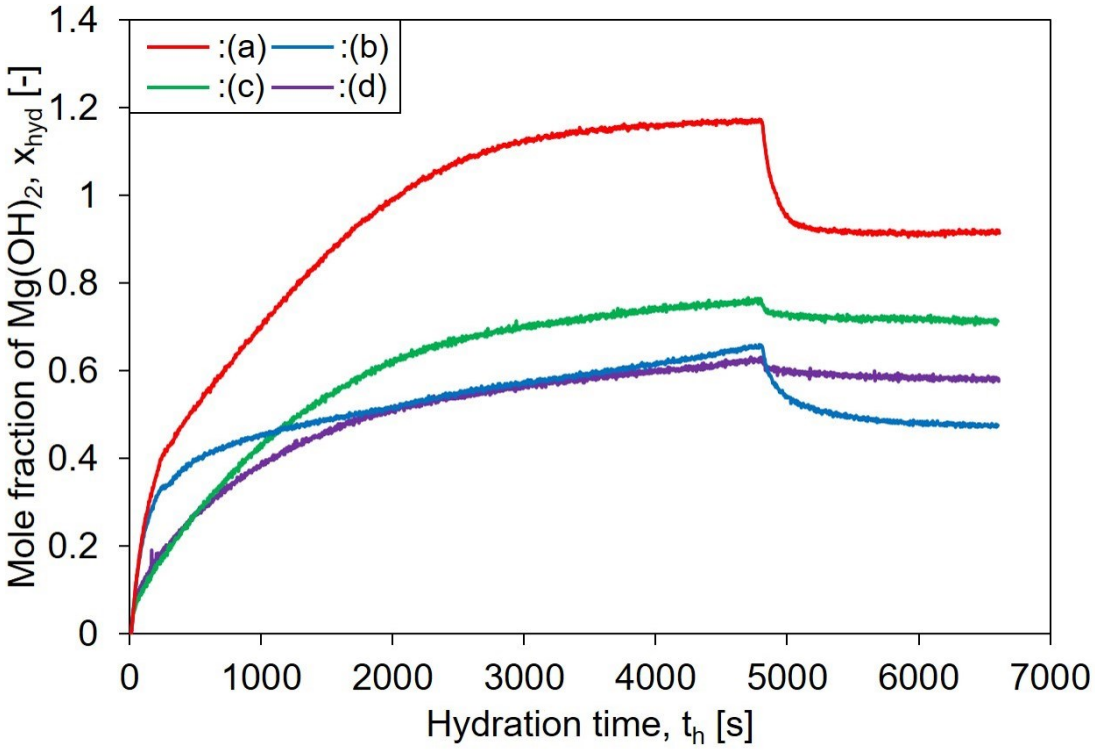

Figure S11. Hydration behavior of (a) de-L10/LO10, (b) de-L10, (c) de-LO20, and (d) de-$Mg(OH)_2$-W (110 ℃; 31.2 kPa). $Mg(OH)_2$-W, L10, LO20, and L10/LO10 were dehydrated at a temperature of 350 ℃, following which they were hydrated at 110 ℃ (P_{H2O}: 31.2 kPa).

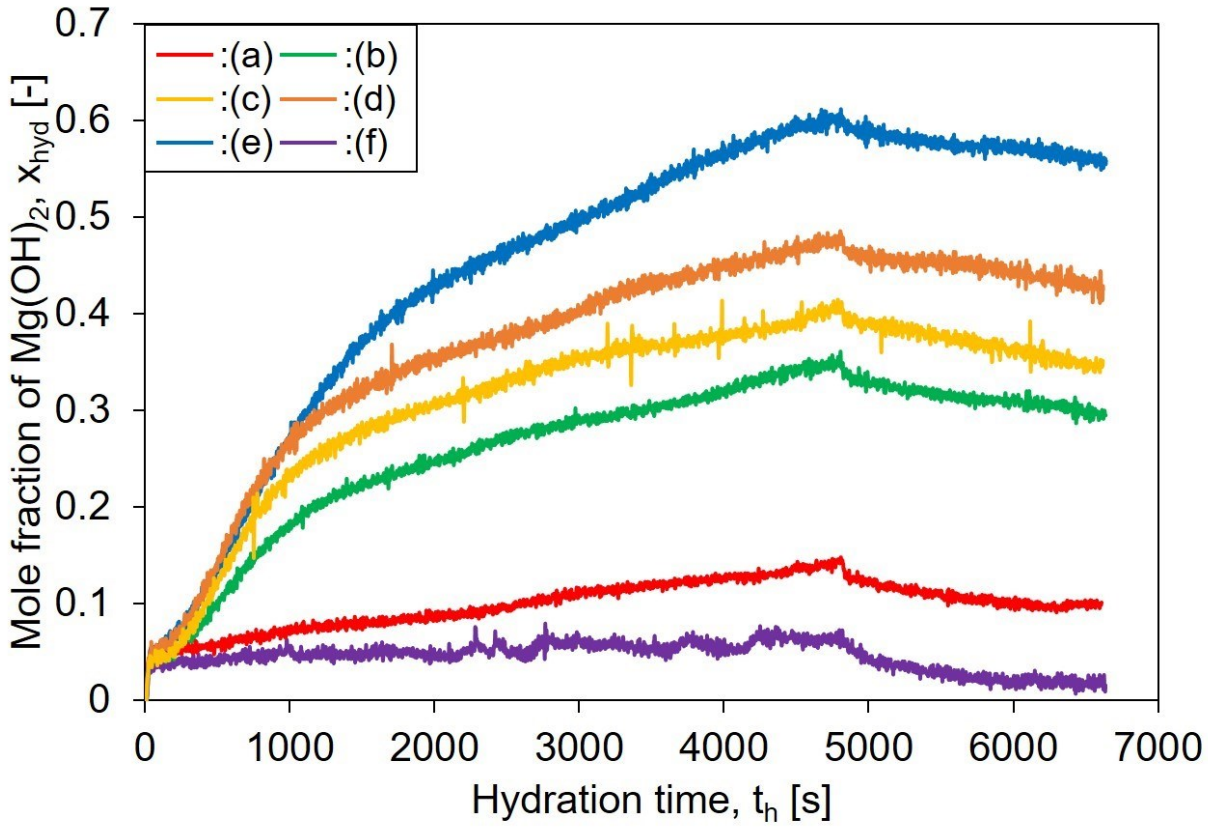

Figure S12. Hydration behavior of pure and LiOH-added MgO studied at 200 ℃ for (a) de-LO10, (b) de-LO20, (c) de-LO25, (d) de-LO30, (e) de-LO50, and (f) de-$Mg(OH)_2$-W. LO10, LO20, LO25, LO30, LO50, and $Mg(OH)_2$-W were dehydrated at a temperature of 350 ℃, following which they were hydrated at a temperature of 200 ℃ (P_{H2O}: 57.8 kPa). LO10, LO20, LO25, LO30, and LO50 represent LiOH-added $Mg(OH)_2$ samples where the $Mg(OH)_2$:LiOH molar ratios were 100:10, 100:20, 100:25, 100:30, and 100:50, respectively.

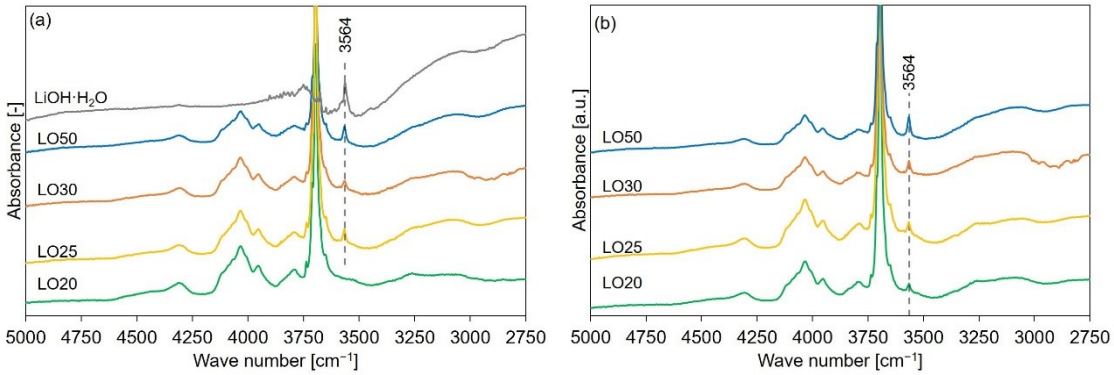

Figure S13. FT-IR spectral profiles recorded for samples (as-synthesized LO20, LO25, LO30, and LO50) prepared following the (a) impregnation method and (b) physical mixing technique. LO20, LO25, LO30, and LO50 represent LiOH-added $Mg(OH)_2$ samples where the $Mg(OH)_2$:LiOH molar ratios were 100:20, 100:25, 100:30, and 100:50, respectively.

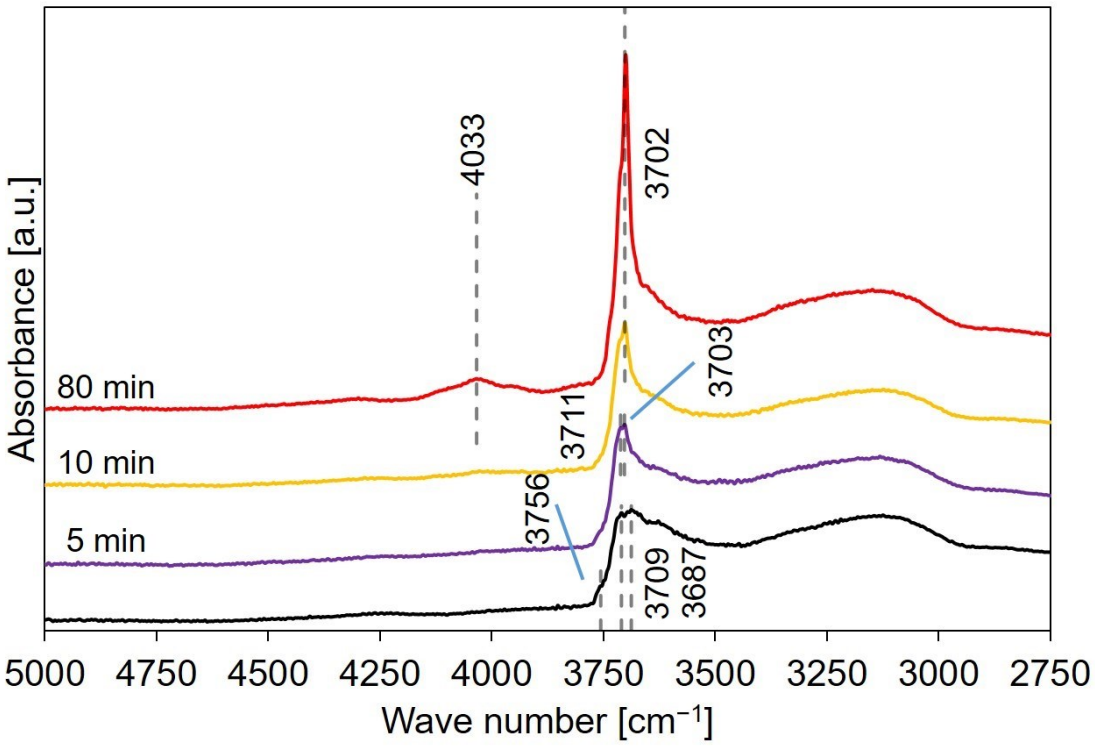

Figure S14. FT-IR spectral profiles recorded for de-MgO-W hydrated at 110 ℃ (P_{H2O}: 31.2 kPa). MgO-W was dehydrated at a temperature of 350 ℃, following which it was hydrated at 110 ℃ (P_{H2O}: 31.2 kPa).

Table S1. Hydration conversion values recorded at a temperature of 200 ℃ for de-$Mg(OH)_2$-W and LiOH/MgO. LO10, LO20, LO25, LO30, and LO50 represent LiOH-added $Mg(OH)_2$ samples where the $Mg(OH)_2$:LiOH molar ratio were 100:10, 100:20, 100:25, 100:30, and 100:50, respectively.

Sample	Hydration conversion (Δx_1) [%]
de-$Mg(OH)_2$-W	2.9
de-LO10	10.8
de-LO20	31.7
de-LO25	38.1
de-LO30	45.3
de-LO50	58.3